ELSEVIER

Aerosol Science 35 (2004) 135–139

Journal of
Aerosol Science

www.elsevier.com/locate/jaerosci

Particle density inferred from simultaneous optical and aerodynamic diameters sorted by composition

D.M. Murphy[a,*], D.J. Cziczo[a,b], P.K. Hudson[a,b], M.E. Schein[a,b], D.S. Thomson[a,b]

[a] *Aeronomy Laboratory, National Oceanic and Atmospheric Administration, NOAA, Mail Stop R-AL6 325 Broadway, Boulder, CO 80305, USA*

[b] *Cooperative Institute for Research in the Environmental Sciences, University of Colorado, USA*

Received 10 April 2003; received in revised form 14 July 2003; accepted 16 July 2003

Abstract

On the same atmospheric particles, we have measured the aerodynamic diameter, the height of the scattered light pulse to estimate the optical diameter, and the composition with a laser ionization mass spectrometer. Different types of particles, as determined by the mass spectra, have distinct relationships between optical and aerodynamic diameters. The relative densities of organic and sulfate particles inferred from the aerodynamic and optical diameters are consistent with the composition inferred from the mass spectra.
© 2003 Elsevier Ltd. All rights reserved.

Keywords: Aerodynamic diameter; Optical diameter; Density; Aerosol; Particle composition

Experimental

The particle analysis by laser mass spectrometry (PALMS) instrument, which collects mass spectra of the ions produced from single particles, has been described previously (Murphy & Thomson, 1995; Thomson, Schein, & Murphy, 2000). A second continuous laser beam and scattered light collection has been added to the instrument to provide aerodynamic sizing of particles (Wilson & Liu, 1980; Prather, Nordmeyer, & Salt, 1994). A 50% beamsplitter was used to separate the 532 nm laser beam into two beams 3.3 cm apart. Light scattered as a particle transits the first laser beam is collected by an ellipsoidal mirror over a range of about 17–64° from forward scattering. Light scattered as a particle transits the second laser beam is collected with varying efficiency between 25° and 155°.

* Corresponding author. Tel.: +1-303-497-5640; fax: +1-303-497-5373.
E-mail address: dmurphy@al.noaa.gov (D.M. Murphy).

0021-8502/$ - see front matter © 2003 Elsevier Ltd. All rights reserved.
doi:10.1016/S0021-8502(03)00386-0

Collection of light from both beams has a complicated angular pattern and a polarization dependence because the mirrors have cutouts for the particle beam and mounting hardware. The mirrors for the second laser beam are also shaped to serve as ion extraction plates (Fig. 2, Murphy & Thomson, 1995). The light scattering signals from both photomultipliers (Hamamatsu 5600) are amplified, then added with a transformer and digitized to 8 bits (Acqiris DP105). The resulting signal shows both pulses and their separation. The pulse spacing and heights are determined in software.

Particles were introduced into the vacuum system using a focusing inlet based on Schreiner, Schild, Voigt, and Mauersberger (1999). This inlet was controlled at about 50 mbar so the transmission characteristics of the inlet did not change with outside pressure. Light scattering pulse heights are taken from the second beam because only that beam was automatically realigned about every 30 min during airborne measurements.

Aerodynamic diameters

Aerodynamic diameters of ambient particles were determined from the transit time between the laser beams. Calibrations were performed using polystyrene latex spheres covering a diameter range of 0.16–1.03 μm and a pressure range of 20–60 mbar for selected sizes. Because the inlet was operated at low pressure, the density dependence of the aerodynamic diameter is somewhat different than for inlets operated at atmospheric pressure. The aerodynamic behavior of a particle exiting a nozzle is determined by the Stokes number:

$$Stk = \frac{\rho C d^2 v_g}{9\mu D},$$

where ρ is the density, C the Cunningham slip correction, d the particle diameter, v_g the gas velocity, μ the gas viscosity, and D the inlet diameter.

At atmospheric pressure, particles in our size range are larger than the mean free path and the slip correction factor is nearly constant, leading to a proportionality

$$d_{aero} \alpha d_{geom} \rho^{0.5}.$$

At 40 mbar, however, the mean free path is about 1.6 μm. The slip correction for sub-micron particles is then proportional to the diameter and the functional dependence on density changes to

$$d_{aero} \alpha d_{geom} \rho.$$

The calibrations showed a small (few percent) effect of pressure that was not accounted for with the Stokes number. This departure from the solution being described by a single dimensionless parameter could be due either to fluid drag downstream of the inlet or the changing Reynolds number in the inlet as the pressure is changed.

A full calculation shows that for our conditions a density change of a factor of 1.7 leads to a change in aerodynamic diameter of between 1.65 and 1.7, depending on the particle size and pressure. The results presented here use the full calculation at different densities for each particle with a correction for the non-Stokes-number pressure dependence.

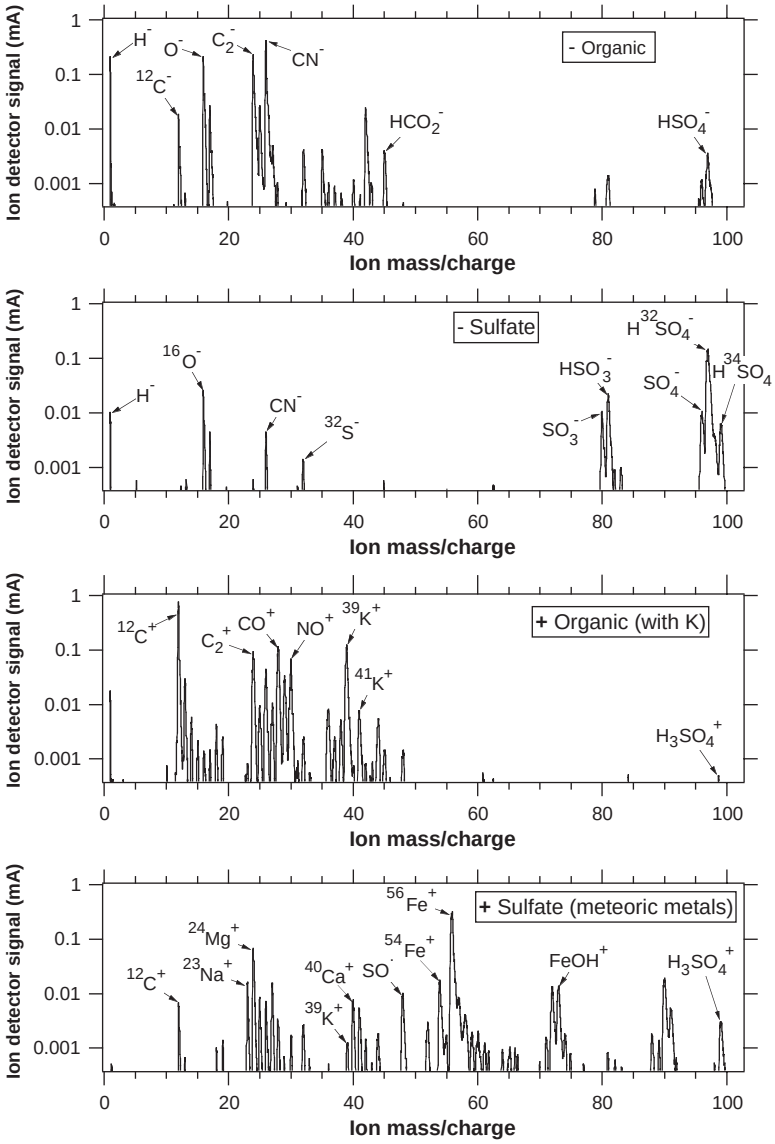

Fig. 1. Examples of the types of mass spectra identified as organic and sulfate particles in negative and positive ion modes. Metals produce positive ions much more easily than sulfuric acid, so much so that laboratory calibrations have shown that the large Mg and Fe peaks in the bottom panel each represent less than 1% of the particle mass and these particles are $>95\%$ sulfuric acid and water (Cziczo, Thomson, & Murphy, 2001).

Results

The data shown are based on mass spectra of particles acquired while flying on the WB-57F aircraft during July 2002 from Key West, Florida. Over 14,000 mass spectra were acquired during the flights. These mass spectra were grouped using cluster analysis (Murphy, Middlebrook, & Warshawsky,

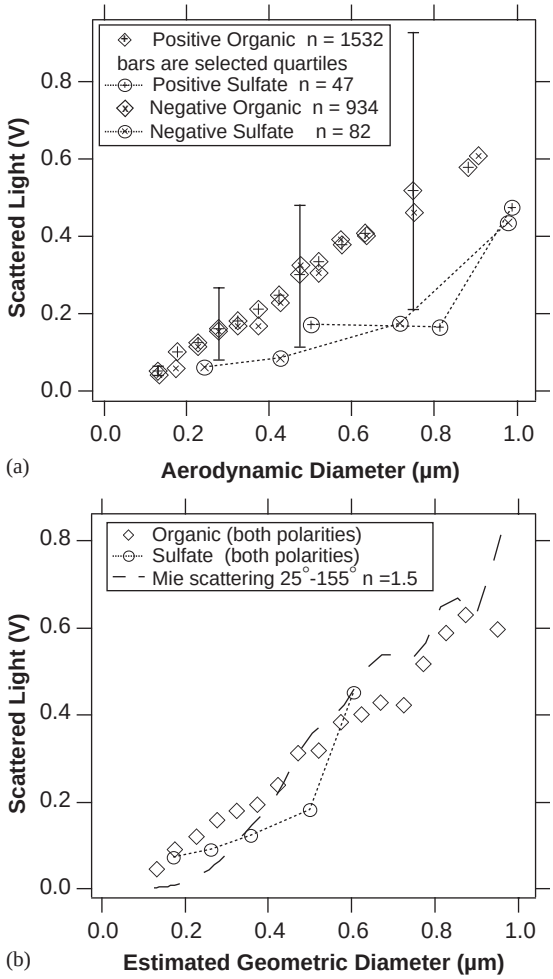

Fig. 2. (a) The average light scattered as a function of the aerodynamic diameter (density $= 1\ \mathrm{g\,cm^{-3}}$) for the types of particles shown in Fig. 1. The agreement between the positive and negative ion curves shows that the identification of organic and sulfate particles is consistent for both polarities. (b) The diameters of the sulfate particles have been recalculated assuming a density of $1.7\ \mathrm{g\,cm^{-3}}$. The agreement between the organic and sulfate curves shows that their densities are consistent with the composition inferred from the mass spectra.

2003) and two sets of clusters were considered: those with the highest organic content and those with the highest sulfate content. Average mass spectra from organic and sulfate clusters are shown in Fig. 1. In order to simplify the range of possible types of particles, only particles from above 11 km altitude were considered for further analysis. At these altitudes, the positive ion sulfate data cluster contained meteoric metals, showing that the particles had come from the stratosphere and hence were probably sulfuric acid rather than ammonium sulfate.

Fig. 2 shows the average light scattered for each type of particle as a function of the aerodynamic diameter. Quartiles (enclosing half the data) are shown for selected points. The wide spreads are because the mass spectrometer does not employ sheath air or other techniques commonly used in

optical particle counters to keep particles from being undersized at the edges of the laser beams. After averaging, however, there is excellent agreement between the positive and negative spectra, showing that the choice of sulfate and organic particles is consistent for both polarities. The sulfate and organic particles have distinct relationships between aerodynamic diameter and scattering. The reason is that the density enters into the aerodynamic diameter and the refractive index enters into the light scattering. The refractive index of stratospheric sulfuric acid/water solutions (about 1.5) is similar to that of many plausible organic species. However, the densities are quite different (about 1.7 and 1, respectively). Fig. 2b shows the traces shifted with the aerodynamic diameters calculated with those densities. The good match shows consistency between the aerodynamic, optical, and composition.

Also shown on Fig. 2 is a Mie scattering calculation for 25° and 155°. Scattering from the more efficiently collected polarization (S1) has been scaled to match the data. Except for the smallest particles, both curves have about the predicted functional relationship over this size range. The smallest particles appear to scatter more light than predicted because only those that scatter the most light (e.g. those in the middle of the laser beam) are detected, biasing the measurements high. A small amount of absorbing material may be present in some of the organic particles that originated from biomass burning, but Mie scattering calculations show that an imaginary index of 0.02 changes the light scattering by less than 20% between 0.2 and 0.8 μm, mostly as a decrease in scattering for the larger particles.

Particle densities have been retrieved from aerodynamic and optical diameters using separate instruments (Hand & Kreidenweis, 2002) as well as instrumentation designed to measure density (McMurry, Wang, Park, & Ehara, 2002). The results shown here benefit from measuring both aerodynamic and optical diameters on the same particles. Even without mass spectra to sort the particles, recording the pulse height in traditional aerodynamic sizing instruments may provide additional information on the particles with minimal extra hardware.

References

Cziczo, D. J., Thomson, D. S., & Murphy, D. M. (2001). Ablation, flux, and atmospheric implications of meteors inferred from stratospheric aerosol. *Science*, *291*, 1772–1775.

Hand, J. L., & Kreidenweis, S. M. (2002). A new method for retrieving particle refractive index and effective density from aerosol size distribution data. *Aerosol Science and Technology*, *36*, 1012–1026.

McMurry, P. H., Wang, X., Park, K., & Ehara, K. (2002). The relationship between mass and mobility for atmospheric particles: A new technique for measuring particle density. *Aerosol Science and Technology*, *36*, 227–238.

Murphy, D. M., Middlebrook, A. M., & Warshawsky, M. (2003). Cluster analysis of data from the particle analysis by laser mass spectrometry (PALMS) instrument. *Aerosol Science and Technology*, *37*, 382–391.

Murphy, D. M., & Thomson, D. S. (1995). Laser ionization mass spectroscopy of single aerosol particles. *Aerosol Science and Technology*, *22*, 237–249.

Prather, K. A., Nordmeyer, T., & Salt, K. (1994). Real-time characterization of individual aerosol particles using time-of-flight mass spectrometry. *Analytical Chemistry*, *66*, 1403–1407.

Schreiner, J., Schild, U., Voigt, C., & Mauersberger, K. (1999). Focusing of aerosols into a particle beam at pressures from 10 to 150 Torr. *Aerosol Science and Technology*, *31*, 373–382.

Thomson, D. S., Schein, M. E., & Murphy, D. M. (2000). Particle analysis by laser mass spectrometry WB-57F instrument overview. *Aerosol Science and Technology*, *33*, 153–169.

Wilson, J. C., & Liu, B. Y. H. (1980). Aerodynamic particle-size measurements by laser-doppler velocimetry. *Journal of Aerosol Science*, *11*, 139–150.